From CA to Gene Expression: Machines and Mechanisms

Debashish Chowdhury[1], Ashok Garai[1], Philip Greulich[2], Katsuhiro Nishinari[3], Andreas Schadschneider[2], Tripti Tripathi[1], and Jian-Sheng Wang[4]

[1] Physics Department, Indian Institute of Technology, Kanpur 208016, India
[2] Institute for Theoretical Physics, University of Cologne, 50937 Köln, Germany
[3] Department of Aeronautics and Astronautics, School of Engineering, University of Tokyo, Hongo, Bunkyo-ku, Tokyo 113-8656, Japan
[4] Department of Physics, National University of Singapore, Singapore 117542, Singapore

Abstract. Molecular motors are proteins or macromolecular complexes which use input energy to perform mechanical work. Some of these motors move on filamentous proteins whereas other move on DNA or RNA strands. Often, many such motors move simultaneously on the same track and their collective movement is similar to vehicular traffic on highways. We have developed theoretical models of different types of molecular motor traffic by appropriately extending the totally asymmetric simple exclusion process (TASEP). Thus, our models of molecular motor traffic belong to the broad class of driven-diffusive lattice gas models which have close relations with cellular automata. By drawing analogy with vehicular traffic, we have introduced novel quantities for characterizing the nature of the spatio-temporal organization of molecular motors on their tracks. We show how the mechano-chemistry of the individual motors influence the traffic-like intracellular collective phenomena.

1 Introduction

Motility is the hallmark of life. Most of the motions of animals and plants arise from movements at the molecular level which are driven by motor proteins. A key feature of molecular motor transport is that the motor proteins move on filamentous "tracks" [1,2,3,4]. The tracks for motor proteins are made of either proteins or nucleic acids (e.g., DNA or RNA). A common feature of all these motors is that these perform mechanical work by utilizing some other form of input energy and hence the name "motor". All the molecular motors we consider in this paper directly convert chemical energy into mechanical work.

During several biological processes many motors move simultaneously on the same track. The collective movement of the motors under such cicumstances strongly resemble vehicular traffic flow [5,6]. Our aim is to analyze molecular motor traffic from the perspective of vehicular traffic [7,8]. In the "particle-hopping" models of vehicular traffic each vehicle is represented by a particle and the dynamics of the system is formulated in terms of "rules" which are

H. Umeo et al. (Eds): ACRI 2008, LNCS 5191, pp. 1–10, 2008.

reminiscent of the update rules of cellular automata (CA). To our knowledge, the totally asymmetric simple exclusion process (TASEP) [9] is the simplest model of a system of interacting self-propelled particles on a discrete lattice. It has been extended in several ways to formulate "particle-hopping" models for capturing various interesting aspects of vehicular traffic [7]. Our models of molecular motor traffic may be regarded as biologically motivated extensions of TASEP. In all the examples of molecular motor traffic considered in this paper, the states of the system (both position and chemical states) are represented by discrete variables. In the analytical formulation of our theories, time is treated as a continuous variable, whereas discretization of time is needed not only for the numerical integration of the equations of motion, but also for computer simulations of these models.

2 Traffic of Kinesins on Microtubule Track: Change of Lane?

The members of the *kinesin* superfamily of cytoskeletal motors move on microtubules (MT). These motors run on chemical fuel in the sense that the mechanical energy required for their movement is supplied from the energy released when adenosine triphosphate (ATP) is hydrolyzed to adenosine diphosphate (ADP) [4].

We have focussed attention on a family of single-headed kinesins, called KIF1A. Our original model (from now onwards, we shall refer to it as the NOSC model) [10,11] captures the essential steps of the mechano-chemical cycle of individual KIF1A motors as well as steric interactions on the same track. Normally, a single microtubule consists of thirteen protofilaments each of which is analogous to a "lane" for the molecular motors. Recently we have extended the NOSC model [12] by allowing additional processes which correspond to lane changing, i.e., allowing a motor to shift from one protofilament to a neighbouring one on the same MT.

The equispaced binding sites for KIF1A on a given protofilament of the MT are labelled by the integer index i ($i = 1, ..., L$). We use the integer index j to label the protofilaments; the position of each binding site is denoted completely by the pair (i, j). We impose periodic boundary conditions along both the i- and j-directions.

A single biochemical cycle of a KIF1A motor consists of a sequence of four states, namely, kinesin (K), kinesin bound with ATP (KT), kinesin bound with ADP and phosphate (KDP) and, finally, kinesin bound with only ADP (KD). The motor binds strongly to the MT track in both the states K and KT; the state KDP has very short life time and KD binds weakly to the track. Therefore, at each spatial location in our simplified model, a KIF1A is allowed to exist in one of the two distinct "chemical" states depending on whether it is bound strongly or weakly to the track; these two chemical states are denoted by the symbols S and W, respectively.

The allowed transitions and the corresponding rate constants are shown in fig.1. The rate constants ω_a and ω_d account for the attachments and detachments of the motors. The rate constant ω_b corresponds to the unbiased one-dimensional Brownian motion of the motor in the state where it is weakly bound to the

MT track. The rate constant ω_h is associated with the process driven by ATP hydrolysis which causes the transition of the motor from the state S to the state W. The rate constants ω_f and ω_s, together, capture the Brownian ratchet mechanism of movement of a KIF1A motor [10,11].

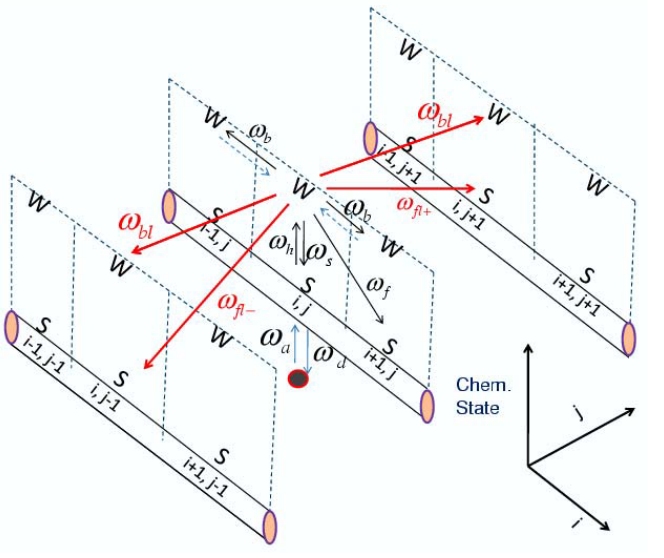

Fig. 1. A schematic description of the mechano-chemical cycle of a single-headed kinesin motor KIF1A in our extended model where lane changings are allowed. The equispaced sites labelled by the integers $..., i-1, i, i+1, ...$ denote the binding sites of the motor on a given protofilament of the microtubule (MT) track while the integer index j labels the protofilaments. The symbols S and W denote the two "chemical" states of the motor in which it is, respectively, strongly and weakly bound to the track. The allowed transitions are indicated by the arrows and the symbols accompanying the arrows are the corresponding rate constants.

The rules of time evolution in the extended NOSC model proposed in ref.[12] are identical to those in the NOSC model, except for the following additional lane-changing rules (see fig.1):

A motor weakly-bound (i.e., in state W) to the binding site i on the protofilament j is allowed to move to the positions $(i, j+1)$ and $(i, j-1)$

(i) *without* simultaneous change in its chemical state, both the corresponding rates being ω_{bl};
(ii) *with* simultaneous transition to the chemical state S, the corresponding rate constants being ω_{fl+} and ω_{fl-}, respectively.

As in the earlier TASEP-type models of cytoskeletal motor traffic [13,14,15,16,17,18], none of the lattice sites is allowed to be occupied by more than one motor at a time.

Let $S_i(j,t)$ and $W_i(j,t)$ denote the probabilities for a motor to be in the "chemical" states S and W, respectively, at site i on the protofilament j. In the extended NOSC model, under mean-field approximation, the master equations for the probabilities $S_i(j,t)$ and $W_i(j,t)$ are given by

$$\begin{aligned}\frac{dS_i(j,t)}{dt} &= \omega_a[1-S_i(j,t)-W_i(j,t)] - \omega_h S_i(j,t) - \omega_d S_i(j,t) + \omega_s W_i(j,t) \\ &+\omega_f W_{i-1}(j,t)[1-S_i(j,t)-W_i(j,t)] \\ &+\omega_{fl+}[W_i(j-1,t)][1-S_i(j)-W_i(j)] \\ &+\omega_{fl-}[W_i(j+1,t)][1-S_i(j)-W_i(j)], \end{aligned} \tag{1}$$

$$\begin{aligned}\frac{dW_i(j,t)}{dt} &= \omega_h S_i(j,t) - \omega_s W_i(j,t) - \omega_f W_i(j,t)[1-S_{i+1}(j,t)-W_{i+1}(j,t)] \\ &-\omega_b W_i(j,t)[2-S_{i+1}(j,t)-W_{i+1}(j,t)-S_{i-1}(j,t)-W_{i-1}(j,t)] \\ &+\omega_b[W_{i-1}(j,t)+W_{i+1}(j,t)][1-S_i(j,t)-W_i(j,t)] \\ &+\omega_{bl}[W_i(j-1,t)+W_i(j+1,t)][1-S_i(j,t)-W_i(j,t)] \\ &-\omega_{bl}W_i(j,t)[2-S_i(j+1,t)-W_i(j+1,t)-S_i(j-1,t) \\ &-W_i(j-1,t)-\omega_{fl+}W_i(j,t)[1-S_i(j+1,t)-W_i(j+1,t)] \\ &-\omega_{fl-}W_i(j,t)[1-S_i(j-1,t)-W_i(j-1,t)]. \end{aligned} \tag{2}$$

Solving these equations analytically, we address a fundamental question: does lane changing increase or decrease flux per lane?

In the steady state under *periodic* boundary conditions, $\tilde{S} = S_i(j,t)$ and $\tilde{W} = W_i(j,t)$, independent of t and irrespective of i and j; from eqs.(1) and (2), we get

$$\tilde{S} = \frac{-\tilde{\Omega}_h - \tilde{\Omega}_s - (\tilde{\Omega}_s - 1)K + \sqrt{\tilde{D}}}{2K(1+K)} \tag{3}$$

$$\tilde{W} = \frac{\tilde{\Omega}_h + \tilde{\Omega}_s + (\tilde{\Omega}_s + 1)K - \sqrt{\tilde{D}}}{2K}, \tag{4}$$

where $K = \omega_d/\omega_a$, $\tilde{\Omega}_h = \omega_h/\tilde{\omega_f}$, $\tilde{\Omega}_s = \omega_s/\tilde{\omega_f}$, with $\tilde{\omega_f} = \omega_f + \omega_{fl+} + \omega_{fl-}$, and

$$\tilde{D} = 4\tilde{\Omega}_s K(1+K) + (\tilde{\Omega}_h + \tilde{\Omega}_s + (\tilde{\Omega}_s - 1)K)^2. \tag{5}$$

The average total density of the motors attached to each filament of the MT in the steady state is given by

$$\rho = \tilde{S} + \tilde{W} = \frac{\tilde{\Omega}_h + \tilde{\Omega}_s + (\tilde{\Omega}_s + 1)K - \sqrt{\tilde{D}} + 2}{2(1+K)}. \tag{6}$$

Using the expressions (3) and (4) for $\tilde{S}$ and $\tilde{W}$, respectively, in the expression

$$J = \omega_f \tilde{W}(1 - \tilde{S} - \tilde{W}) \tag{7}$$

for the flux of KIF1A motors per lane of the MT highway, we get

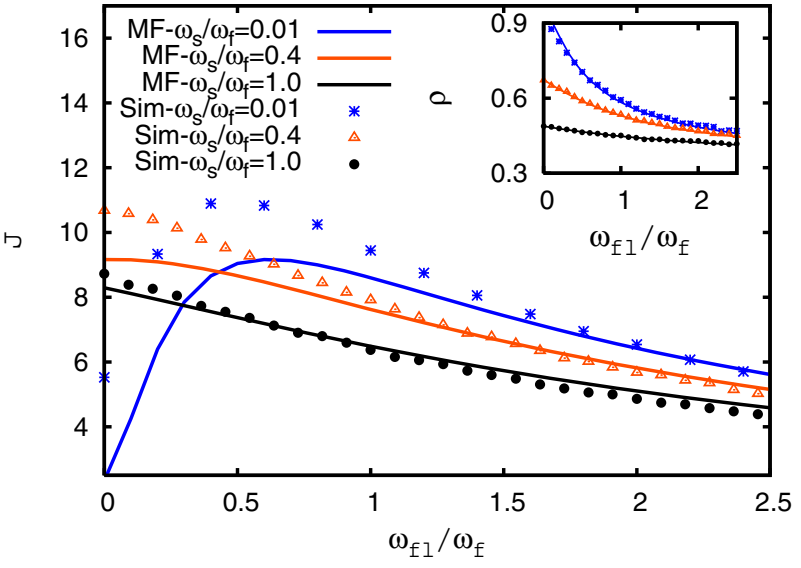

Fig. 2. (Color online) Flux per lane (and, in the inset, average density of the motors on each lane) are plotted against ω_{fl}/ω_f for a few values of ω_s/ω_f. Our mean-field predictions (labelled MF) are plotted by lines while the discrete data points (labelled Sim) have been obtained from our computer simulations of the model.

$$J = \frac{\omega_f \left[K^2 - \left(\tilde{\Omega}_h + (1+K)\tilde{\Omega}_s - \sqrt{\tilde{D}} \right)^2 \right]}{4K(1+K)}. \tag{8}$$

For graphical presentation of our main results, we use the estimates of the rate constants which were extracted earlier [11] from empirical data on single KIF1A (we use $\omega_h = 125\ \mathrm{s}^{-1}$). Since no estimate of ω_{fl+} and ω_{fl-} are available, we use $\omega_{fl+} = \omega_{fl-} = \omega_{fl}$ and vary the single parameter ω_{fl}/ω_f over a wide range to explore the consequences of different rates of lane changing. We have also carried out computer simulations of the extended NOSC model and computed the flux J of the motors per protofilament as well as the average density ρ; a comparison of the predictions of our mean-field theory with these simulation data establishes the level of accuracy of our mean-field theoretical predictions.

In Fig. 2 we plot J (obtained from eqn. (8)) and ρ (given by eqn.(6)) against ω_{fl}/ω_f for several different values of ω_s/ω_f and compare with the corresponding simulation data. When ω_s/ω_f is sufficiently high, the density ρ is small even in the absence of lane changing ($\omega_{fl} = 0$); in that case, the motors feel hardly any steric hindrance. In this regime, increasing ω_{fl}/ω_f of ω_s/ω_f has very little effect on the average speed of the motors; it is the decrease of density that is responsible for the *monotonic* decrease of J with ω_{fl}.

In sharp contrast, at sufficiently low values of ω_s/ω_f, J varies *non-monotonically* with ω_{fl}/ω_f. In this regime of ω_s/ω_f, at $\omega_{fl} = 0$, the high density of ρ causes steric

hindrances which, in turn, leads to small J. When ω_{fl} is "switched on", ρ decreases with increasing ω_{fl} and J increases up to a maximum because of the weakening of the hindrance effects. But, beyond a certain range of ω_{fl}/ω_f, the density of motors becomes so low that the movement of the motors is practically free of mutual hindrance; the decrease of J beyond its maximum is caused by the further reduction of density. Larger difference between the predictions of our approximate analytical calculations and computer simulation data at lower values of ω_s/ω_f arises from the fact that the mean-field approximation neglects correlations which increases with increasing densitity of the motors.

3 Traffic of RNAP Motors on DNA Tracks

The motor RNA polymerase (RNAP) catalyzes the polymerization of a RNA molecule from the corresponding DNA template [19] and the process is called transcription. To our knowledge, almost all the models of transcription available in the literature [20,21,22,23,24,25,26,27,28,29,30,31] capture only the stochastic mechano-chemistry of the individual RNAP motors. The effects of steric interactions of the RNAPs on the rate of RNA synthesis has been modelled only in a recent work by two of us [32,33].

The model reported originally in ref.[32] is described schematically in fig.3. Each lattice site corresponds to a nucleotide on the DNA template. The elongation of the growing RNA by one nucleotide leads to a forward stepping of the RNAP by one unit. A mechano-chemical cycle of the RNAP during elongation of RNA consists of the following major steps: (i) Nucleoside triphosphate (NTP) binding to the active site of the RNAP, (ii) NTP hydrolysis, (iii) release of pyrophosphate (PP_i) (which is produced by the hydrolysis of NTP), and (iv) simultaneous forward stepping of the RNAP. Since PP_i-release is known to be the rate-limiting step, we consider only two distinct chemical states μ of the RNAP; $\mu = 1$ refers to the state in which the RNAP is not bound to any PP_i whereas $\mu = 2$ corresponds to the state with bound PP_i.

The processes corresponding to the rate constants ω_{12} and ω_{21} correspond to PP_i-release and its reverse reaction. The symbol ω_{21}^f is the rate of addition of one NTP to the elongating RNA whereas ω_{12}^b is that of the reverse reaction. The remaining four rate constants, namely, ω_{11}^f, ω_{11}^b, ω_{22}^f, and ω_{22}^b correspond to polymerization/depolymerization of the RNA, by one monomer, unaided by the RNAP. Normally, a single RNAP is large enough to cover $r(> 1)$ successive nucleotides on the track. Therefore, a lattice site is *occupied* by a RNAP if it coincides with the leftmost of the r sites representing that RNAP while the next $r - 1$ sites on its right are *covered* by the same RNAP. However, each RNAP can move forward or backward by only one site in each time step, irrespective of the numerical value of r. Moreover, forward or backward step of a RNAP is implemented only if the target site is not already covered by any other RNAP. Suppose, the total number of RNAPs on the DNA template is N. Then, $\rho = N/L$ is the *number density* of the RNAPs whereas the *coverage density* $\rho_{cov} = Nr/L$ is the total fraction of the nucleotides covered by all the RNAPs together.

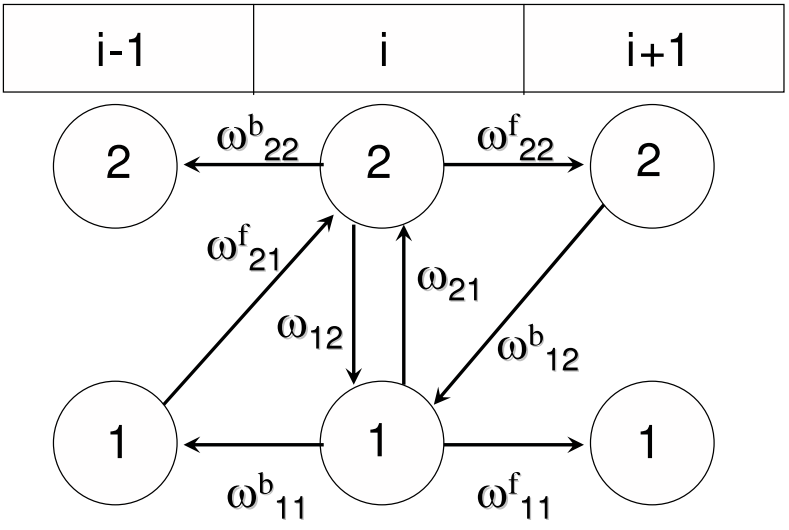

Fig. 3. A schematic representation of the mechano-chemical cycle of each RNAP in the model. The equispaced sites labelled by the integers $..., i-1, i, i+1, ...$ denote the nucleotides on the template DNA track. No PP_i is bound to the RNAP in the state 1 whereas the pyrophosphate (PP_i)-bound state of the RNAP is labelled by the index 2. The allowed transitions denoted by arrows and the corresponding rate constants are also shown.

Let $P_\mu(i,t)$ be the probability that there is a RNAP at the lattice site i and in the chemical state μ at time t. Let $Q(\underline{i}|j)$ be the conditional probability that, given a RNAP at site i, site j is empty. In the mean-field approximation, the master equations for $P_\mu(i,t)$ are given by [32]

$$\begin{aligned}
\frac{dP_1(i,t)}{dt} &= \omega_{11}^f\ P_1(i-1,t)\ Q(\underline{i-1}|i-1+r) \\
&+\ \omega_{11}^b\ P_1(i+1,t)\ Q(i+1-r|\underline{i+1}) \\
&+\ \omega_{12}^b\ P_2(i+1,t)\ Q(i+1-r|\underline{i+1}) \\
&+\ \omega_{12}\ P_2(i,t) -\ \omega_{21}\ P_1(i,t) \\
&-\ (\omega_{11}^f + \omega_{21}^f)\ P_1(i,t)\ Q(\underline{i}|i+r) \\
&-\ \omega_{11}^b\ P_1(i,t)\ Q(i-r|\underline{i})
\end{aligned} \tag{9}$$

$$\begin{aligned}
\frac{dP_2(i,t)}{dt} &= \omega_{22}^f\ P_2(i-1,t)\ Q(\underline{i-1}|i-1+r) \\
&+\ \omega_{22}^b\ P_2(i+1,t)\ Q(i+1-r|\underline{i+1}) \\
&+\ \omega_{21}^f\ P_1(i-1,t)\ Q(\underline{i-1}|i-1+r) \\
&+\ \omega_{21} P_1(i,t) -\ \omega_{12}\ P_2(i,t) \\
&-\ (\omega_{22}^b + \omega_{12}^b)\ P_2(i,t)\ Q(i-r|\underline{i}) \\
&-\ \omega_{22}^f\ P_2(i,t)\ Q(\underline{i}|i+r)
\end{aligned} \tag{10}$$

In the steady state under periodic boundary conditions,

$$P_1 = \left(\frac{\omega_{12} + \omega_{12}^b Q}{\Omega_\updownarrow + \Omega_\leftrightarrow Q} \right) \rho$$
$$P_2 = \left(\frac{\omega_{21} + \omega_{21}^f Q}{\Omega_\updownarrow + \Omega_\leftrightarrow Q} \right) \rho \tag{11}$$

where

$$\Omega_\updownarrow = \omega_{12} + \omega_{21}$$
$$\Omega_\leftrightarrow = \omega_{21}^f + \omega_{12}^b \tag{12}$$

and Q is given by

$$Q(\underline{i}|i+r) = Q(i|\underline{i+r}) = \frac{1-\rho r}{1+\rho-\rho r} \tag{13}$$

The corresponding steady-state flux is given by

$$J = \Omega_1 P_1 Q + \Omega_2 P_2 Q$$
$$= (\Omega_1 P_1 + \Omega_2 P_2) \left(\frac{1-\rho_{cov}}{1+\rho-\rho_{cov}} \right) \tag{14}$$

where

$$\Omega_1 = \omega_{11}^f + \omega_{21}^f - \omega_{11}^b$$
$$\Omega_2 = \omega_{22}^f - \omega_{12}^b - \omega_{22}^b, \tag{15}$$

are two *effective forward hopping rates* from the states 1 and 2, respectively.

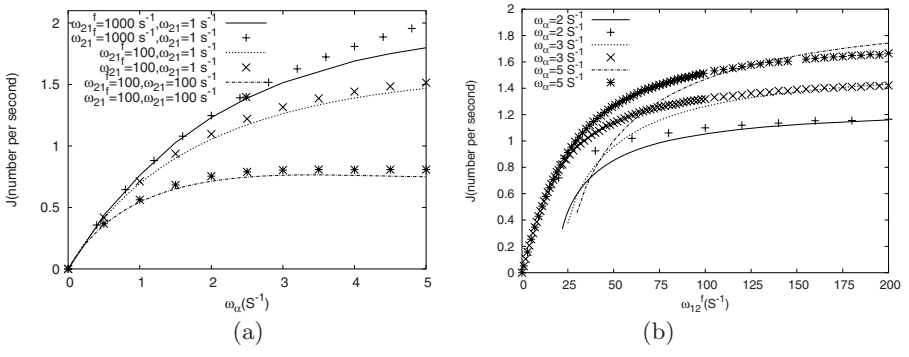

Fig. 4. The steady-state flux of the RNAPs, under open boundary conditions, plotted as a function of (a) ω_α, for three sets of values of the pair of parameters [NTP], [PP$_i$]; (b) ω_{21}^f for three values of the parameter ω_α. The lines correspond to our mean-field theoretic predictions whereas the discrete data points have been obtained from computer simulations.

However, for modeling transcription, open boundary conditions are more realistic than periodic boundary conditions. It is not difficult to write down the counterparts of the equations (10) and (11) under open boundary conditions, but cannot be solved analytically. Solving these equations numerically in the steady state, the numerical estimates of the flux and the average density profile were predicted [32]. These mean-field theoretic estimates are plotted as functions of ω_α and ω_{21}^f, respectively, in figs.4(a) and (b). In the same figure, the corresponding simulation data are also plotted for comparison. The trends of variation of the flux and the average density profile indicate a transition from the low-density phase to the maximal current phase in fig.4(a) and from the high-density phase to the maximal current phase in fig.4(b) [9].

4 Conclusion

In this article we have presented two examples of molecular motor traffic which have been modelled using the language of driven-diffusive lattice gases. Historically, however, first attempt in this direction was made in the context of traffic of ribosomes on a messenger RNA (mRNA) strand during translation of genetic message was developed [34,35,36,37,38,39,40,41,42,43,44,45]. Very recently, such models have been made more realistic by incorporating the mechano-chemistry of individual ribosomes [46,47] in the same spirit in which the models of RNAP traffic have been developed. It would be interesting to develop similar models for traffic-like collective phenomena exhibited by unicellular organisms.

This work is supported (through DC) by a research grant from CSIR (India).

References

1. Howard, J.: Mechanics of Motor Proteins and the Cytoskeleton. Sinauer Associates (2001)
2. Schliwa, M. (ed.): Molecular Motors. Wiley-VCH, Chichester (2002)
3. Kolomeisky, A.B., Fisher, M.E.: Annual Review of Physical Chemistry. 58, 675 (2007)
4. Hackney, D.D., Tamanoi, F.: The Enzymes, vol. XXIII. Elsevier, Amsterdam (2004)
5. Chowdhury, D., Schadschneider, A., Nishinari, K.: Phys. of Life Rev. 2, 318 (2005)
6. Chowdhury, D., Chakrabarti, B.K., Dutta, A.: Common trends in traffic systems. Physica A 372(1) (2006)
7. Chowdhury, D., Santen, L., Schadschneider, A.: Phys. Rep. 329, 199 (2000)
8. Schadschneider, A.: In: This proceedings
9. Schütz, G.M.: Phase Transitions and Critical Phenomena, vol. 19. Acad. Press (2001)
10. Nishinari, K., Okada, Y., Schadschneider, A., Chowdhury, D.: Phys. Rev. Lett. 95, 118101 (2005)
11. Greulich, P., Garai, A., Nishinari, K., Schadschneider, A., Chowdhury, D.: Phys. Rev. E. 75, 041905 (2007)
12. Chowdhury, D., Garai, A., Wang, J.S.: Phys. Rev. E. 77(R), 050902 (2008)
13. Lipowsky, R., Klumpp, S., Nieuwenhuizen, T.M.: Phys. Rev. Lett. 87, 108101 (2001)

14. Lipowsky, R., Chai, Y., Klumpp, S., Liepelt, S., Müller, M.J.I.: Physica A. 372, 34 and references therein (2006)
15. Parmeggiani, A., Franosch, T., Frey, E.: Phys. Rev. Lett. 90, 86601 (2003); Phys. Rev. E 70, 046101 (2004)
16. Frey, E., Parmeggiani, A., Franosch, T.: Genome Inf. 15, 46 (2004) and references therein
17. Evans, M.R., Juhasz, R., Santen, L.: Phys. Rev. E. 68, 026117 (2003)
18. Popkov, V., Rakos, A., Williams, R.D., Kolomeisky, A.B., Schütz, G.M.: Phys. Rev. E. 67, 066117 (2003)
19. Bai, L., Santangelo, T.J., Wang, M.D.: Annu. Rev. Biophys. Biomol. Str. 35, 343 (2006)
20. Jülicher, F., Bruinsma, R.: Biophys. J. 74, 1169 (1998)
21. Wang, H.Y., Elston, T., Mogilner, A., Oster, G.: Biophys. J. 74, 1186 (1998)
22. Sousa, R.: Trends in Biochem. Sci. 21, 186 (1996)
23. Guajardo, R., Sousa, R.: J. Mol. Biol. 265, 8 (1997)
24. Guo, Q., Sousa, R.: J. Mol. Biol. 358, 241 (2006)
25. Bai, L., Shundrovsky, A., Wang, M.D.: J. Mol. Biol. 344, 335 (2004)
26. Bai, L., Fulbright, R.M., Wang, M.D.: Phys. Rev. Lett. 98, 068103 (2007)
27. Bar-Nahum, G., Epshtein, V., Ruckenstein, A.E., Rafikov, R., Mustaev, A., Nudler, E.: Cell. 120, 183 (2005)
28. Tadigotla, V.R., Maoileidigh, D.O., Sengupta, A.M., Epshtein, V., Ebright, R.H., Nudler, E., Ruckenstein, A.E.: Proc. Nat. Acad. Sci. USA. 103, 4439 (2006)
29. Yamada, Y.R., Peskin, C.S.: arxiv:q-bio.BM/0603012 (2006)
30. Woo, H.J.: Phys. Rev. E 74, 011907 (2006)
31. Voliotis, M., Cohen, N., Molina-Paris, C., Liverpool, T.B.: Biophys. J. 94, 334–348 (2008)
32. Tripathi, T., Chowdhury, D.: Phys. Rev. E. 77, 011921 (2008)
33. Tripathy, T.: Ph.D. Thesis, IIT Kanpur (in preparation)
34. MacDonald, C., Gibbs, J., Pipkin, A.: Biopolymers. 6, 1 (1968)
35. MacDonald, C., Gibbs, J.: Biopolymers. 7, 707 (1969)
36. Lakatos, G., Chou, T.: J. Phys. A. 36, 2027 (2003)
37. Shaw, L.B., Zia, R.K.P., Lee, K.H.: Phys. Rev. E. 68, 021910 (2003)
38. Shaw, L.B., Sethna, J.P., Lee, K.H.: Phys. Rev. E. 70, 021901 (2004)
39. Shaw, L.B., Kolomeisky, A.B., Lee, K.H.: J. Phys. A. 37, 2105 (2004)
40. Chou, T.: Biophys. J. 85, 755 (2003)
41. Chou, T., Lakatos, G.: Phys. Rev. Lett. 93, 198101 (2004)
42. Schönherr, G., Schütz, G.M.: J. Phys. A. 37, 8215 (2004)
43. Schönherr, G.: Phys. Rev. E 71, 026122 (2005)
44. Dong, J.J., Schmittmann, B., Zia, R.K.P.: J. Stat. Phys. 128, 21 (2007)
45. Dong, J.J., Schmittmann, B., Zia, R.K.P.: Phys. Rev. E. 76, 051113 (2007)
46. Basu, A., Chowdhury, D.: Phys. Rev. E 75, 021902 (2007)
47. Basu, A., Chowdhury, D.: Amer. J. Phys. 75, 931 (2007)